RESEARCH PAPER

Simple Synthesis of Magnetic Nickel Ferrite Nano Composites Containing Luminescence Material Applicable to Identify Heavy Metal Ions

Erfaneh Moghaddasinejad [1] , Gholamreza Nabiyouni [1]*, Davood Ghanbari [2], Atefeh Kiani [1]

[1] *Department of Physics, Faculty of Science, Arak University, Arak, Iran*

[2] *Department of Science, Arak University of Technology, Arak, Iran*

ARTICLE INFO

Article History:
Received 29 November 2021
Accepted 14 March 2022
Published 01 April 2022

Keywords:
Fluorescent sensor
Heavy metal ions
Nanocomposite
Photo luminescent

ABSTRACT

In the current report synthesis soft magnetic nickel ferrite nanoparticles by hydrothermal and microwave method without using any surfactant. At the second step cadmium sulfide photoluminescence nanoparticles first were prepared without applying surfactant and capping agent at water as a green solvent, then effect of natural and chemical surfactants on the morphology and size of nanoparticles was investigated. $NiFe_2O_4$-CdS nanocomposite was synthesized by hydrothermal method. Nanoparticles were entirely characterized using X-ray diffraction pattern, scanning electron microscopy, Fourier transform infrared spectroscopy and vibrating sample magnetometer. $NiFe_2O_4$-CdS nanocomposite shows competent photoluminescence property under ultraviolet irradiation. Our results approve this nanocomposite is a novel sensor for detecting of the toxic heavy metal ions. Among toxic heavy metal ions, harmful influences of lead, cadmium and mercury on human health are well known to cause many sicknesses. In this investigation heavy metals and bacteria have been detected by prepared materials. Fluorescent sensors with high selectivity and sensitivity are considered to be the most suitable sensors for detection of heavy metal ions.

How to cite this article
Moghaddasinejad E , Nabiyouni G , Ghanbari D, Kiani A. Simple Synthesis of Magnetic Nickel Ferrite Nano Composites Containing Luminescence Material Applicable to Identify Heavy Metal Ions. J Nanostruct, 2022; 12(2):414-425. DOI: 10.22052/JNS.2022.02.017

INTRODUCTION

Luminescence emission happens after a suitable material has absorbed energy from a source such as electron beams, ultraviolet or X-ray, chemical reactions, and heat [1]. The energy leads the atoms into an excited state, and then, because excited states are unstable, the atom undergoes next transition, back to its ground state, and the diffused energy is released in the form of either heat or light or both [2,3]. Photoluminescence, which occurs by virtue of electromagnetic radiation, may range from visible light through ultraviolet and X-ray. It has been demonstrated that, in photoluminescence, the wavelength of emitted light is equal to or longer than that of the exciting light. This distinction in wavelength is caused, to non-radiating vibration energy of atoms or ions [4, 5]. The sulfides of zinc (z) and of cadmium (Cd) are the most main basic materials

* *Corresponding Author Email: G-nabiyouni@araku.ac.ir*

of sulfide-type phosphors [6]. II-IV semiconductor nanocrystals are a significant group of materials owing to the direct connection of their electronic and optical attributes with the size of the nano-particles. In special the photoluminescence spectrum of nano-particles develops from the UV to the IR spectral region owing to the size dependence of the energy band gap.

The use of nano-scale photoluminescence development the photoluminescence efficiency, but ultrafine materials can cause irrecoverable environmental danger. Also, reuse of materials saves raw materials. Due to of the nano-material size, separating this particles after end of the reaction by ordinary filtration are impractical. An efficient way to separate of nano-particle is use of the magnetic nano-particles as one part at nanocomposites that containing photoluminescence nano-material. Magnetic nano-particles can remove the problem of photoluminescence separating by using exterior magnetic field [7-10].

Magnetic material such as the ferrites, in addition to the separation of nanoparticles, can develop the photoluminescence performance. Magnetic nanoparticles show superior properties than the bulk state because they demonstrate the effect of quantum restriction. These unique features emerge when the particle size is less critical size [11, 12].

Ferrite, a ceramic material with magnetic attributes those are useful in many types of electronic system. The most important attributes of ferrites include high electrical resistance and high magnetic permeability. Spinel ferrites of general formula AFe_2O_4 are a large group of materials, they are composed of iron oxide and one (or more other) metals in chemical combination. Recently ferrite has receiving great attention due to their wide range of technological applications in various fields such as ferro-fluids, drug delivery, sensors, catalyst and magnetic resonance imaging (MRI) enhancement. Powder of nano sized $NiFe_2O_4$ a beneficial material owing to its high electromagnetic performance, mechanical hardness, highcoercivity, and great chemical stability [12-17].

Toxic heavy metals in industrial effluents include iron, copper, nickel, mercury, cadmium, lead and chromium. Heavy metal pollution is an important problem, as wide heavy metals produce environmental pollution, and their accumulation in the environment a major danger to Organisms health. There is a necessary requirement for a rapid, sensitive and effective method for finding heavy metal in the environment. Among the common systems for detecting heavy metal ions, induction of plasma / atomic or mass emission spectroscopy by atomic absorption spectroscopy are very prevalent. Light adsorption is a very simple and fast method for making sensors. Metal nanoparticles have very strong and desirable adsorption properties in the ultraviolet-visible region of the electromagnetic spectrum. The most important feature of nano-sensors is their very high sensitivity and detection power [18-20].

Escherichia coli are Gram-negative, facultative anaerobic, rod-shaped, coliform bacterium of the genus E. coli that is generally found in the lower intestine of warm-blooded organisms. Most ways to detect bacteria take a long time; detection by sensors with a photoluminescence mechanism can be a suitable way to shorten the detection time [21,22].

This research goal to presentation a method for detects bacteria and heavy material by ultraviolet light radiation. In this work, CdS-$NiFe_2O_4$ nanocomposite was used to detect heavy metal. The nanocomposite prepared in this study can be frequently used to detect.

MATERIALS AND METHODS

Materials

Fe $(NO_3)_3$ $9H_2O$, $NiSO_4$ $6H_2O$, Sodium hydroxide (NaOH), Cd $(NO_3)_2$, Thiourea (CH_4N_2S), distilled water, Grapefruit extract, Cetrimonium bromide (CTAB), Escherichia coli.

Synthesis of $NiFe_2O_4$ nanoparticles

First 1.54 g of Fe $(NO_3)_3.9H_2O$ and 0.5 g of $NiSO_4.6H_2O$ were dissolved in 200 ml of distilled water, and it was mixed on magnetic stirrer for 5 min. Then 18 ml of 1 M aqueous solution of sodium hydroxide was added as precipitator the pH of solution and was fixed to 10. Resultant solution was then transferred to a Teflon-lined stainless steel autoclave and was heated at 180 °C for 8 h.

In synthesis by microwave, NaOH solution (1 M) was then slowly added to the solution under microwave radiations (510 W, 5 min). In both ways obtained precipitate was washed twice with de-ionized water (After each wash, pH checked) and then was dried in oven for 48h.

Synthesis of CdS nanoparticles

First 0.3 g of $Cd(NO_3)_2$ and 0.1 g of Thiourea were dissolved in 200 ml of distilled water, One time without using surfactant and next times using a surfactant (CTAB and again grapefruit as a natural surfactant). Then it was mixed on magnetic stirrer for 20 min. The resultant solution was then transferred to a Teflon-lined stainless steel autoclave and was heated at 200 °C for 12 h. The obtained light yellow precipitate was washed

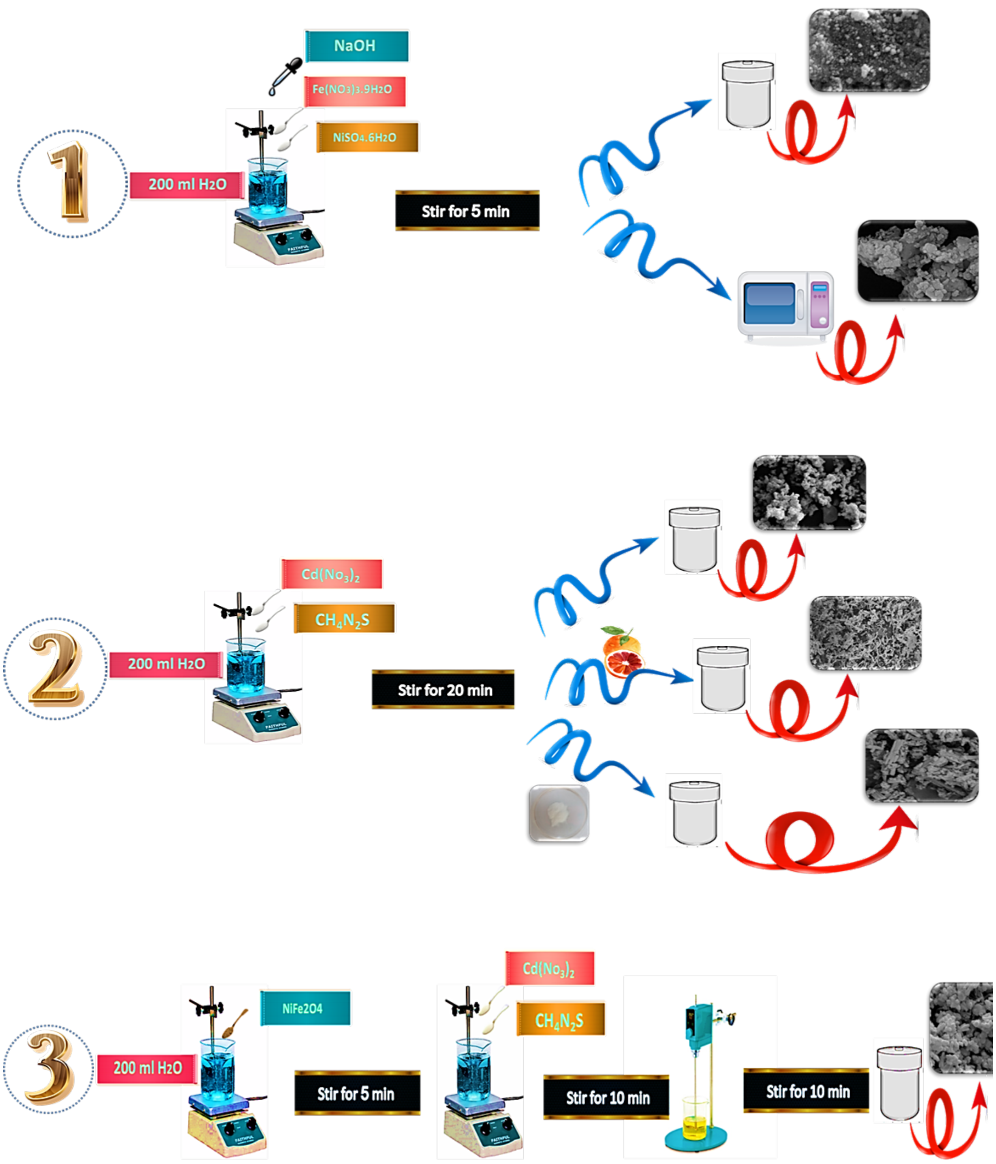

Fig. 1. Schematic of synthesis of $NiFe_2O_4$, CdS and $NiFe_2O_4$-CdS

twice with distilled water. The product then was dried in oven for 20h. CdS nanoparticles were prepared without precipitator using hydrothermal method.

Synthesis of $NiFe_2O_4$-CdS nanocomposites

Firstly 0.1 g of synthesized nickel ferrite was dissolved in 200 ml of distilled water, and it was mixed on magnetic stirrer for 5 min. Then 0.9 g of $Cd(NO_3)_2$ and 0.1 g of Thiourea was added to the solution and was mixed for 10 min and dispersed by mechanical stirrer for 3h. Then transferred to a Teflon-lined stainless steel autoclave and was heated at 200 °C for 12 h. The obtained precipitate was washed. Then product was dried in oven for 20h. Fig. 1 shown the schematic diagram of the preparation steps used in this work.

Methodologies for heavy metal and bacteria detection

First, we examined the photoluminescence (PL) of the cadmium sulfidesolution and CdS-$NiFe_2O_4$ nanocomposites. Next, different concentrations of mercury, lead and bacteria were added to the same solution. Photoluminescence property was examined by luminescence spectrometer.

RESULTS AND DISCUSSION

The crystal structure of the $NiFe_2O_4$-CdS nanocomposites was investigated by XRD pattern and it is depicted in Fig. 2. The pattern illustrates the existence of only single phase of cubic spinel ferrite, which is accordant to JCPDS No 00-003-0875, with Fd-3m space group for nickel ferrite. XRD pattern of CdS that approves suitable agreement with cubic of pure CdS nano-crystal) JCPDS No 00-010-0454). It confirms presence of both phases of $NiFe_2O_4$, and CdS in the pattern. The peak intensities related to each counterpart is relatively similar which is representative of rather equal portion of the shared compounds in the composite.

Fig. 3 and 4 illustrate SEM images of $NiFe_2O_4$ product by hydrothermal and microwave method respectively. The images indicate that the nanoparticles with average diameter size of less than 50 nm were prepared. In the microwave method, the particle size is smaller in comparison to the hydrothermal method.

Effect of surfactant on the morphology and particle size of products under hydrothermal method was investigated. Fig. 5 shows SEM images of cadmium sulfide nanoparticles without

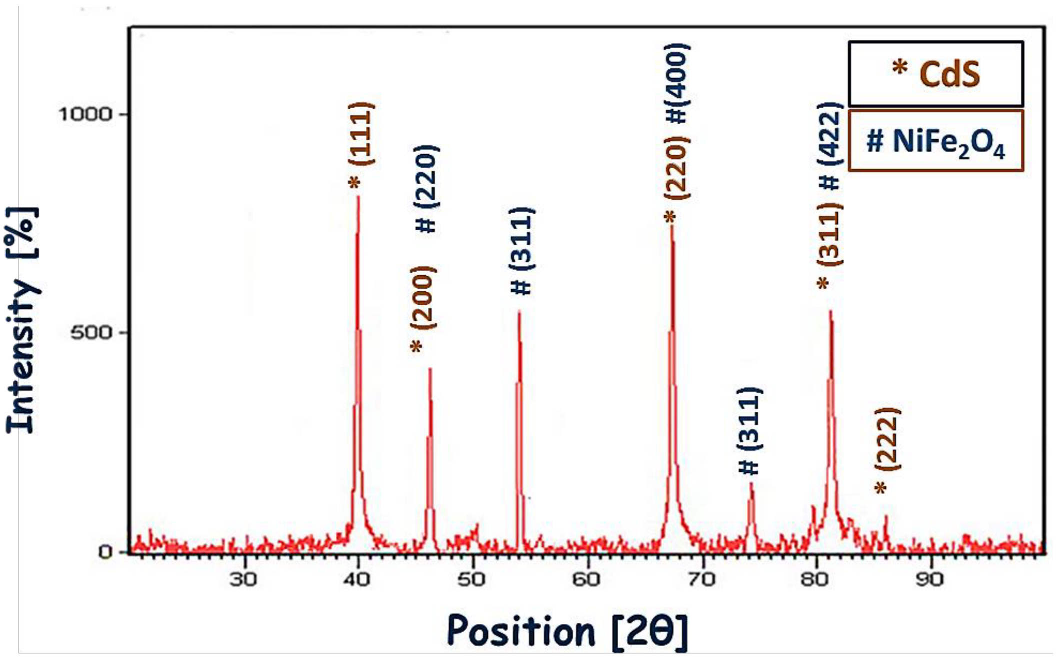

Fig. 2. XRD pattern of a $NiFe_2O_4$ - CdS nanocomposite

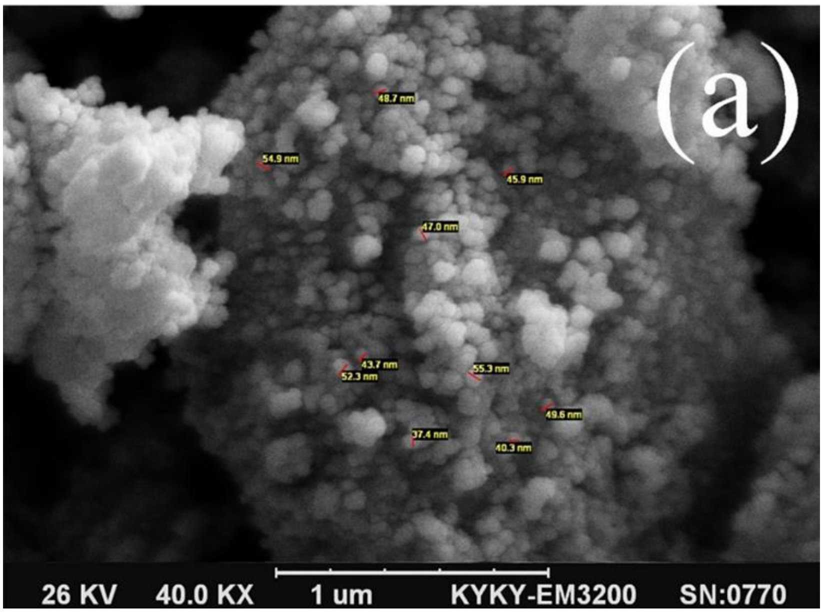

Fig. 3. SEM image of $NiFe_2O_4$ nanoparticles product by hydrothermal method

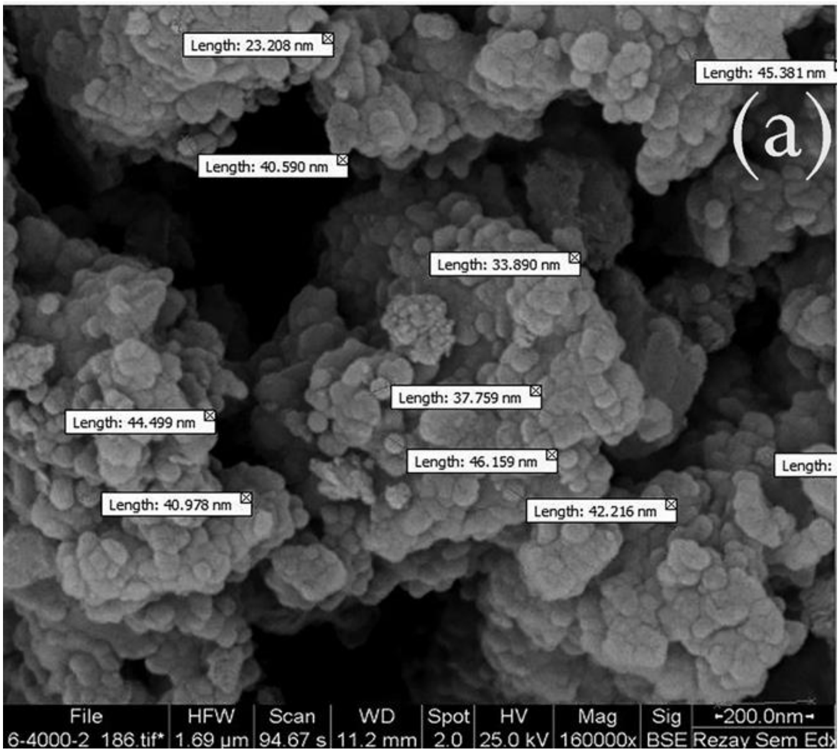

Fig. 4. SEM image of $NiFe_2O_4$ nanoparticles product by microwave method

the use of surfactants .The average particle size of nanoparticles in this sample is less than 50 nm and with a small variation around this value. Fig. 6 shows cadmium sulfide nanoparticles prepared by adding CTAB surfactant and Fig. 7 illustrate SEM images of CdS nanoparticles in the presence of

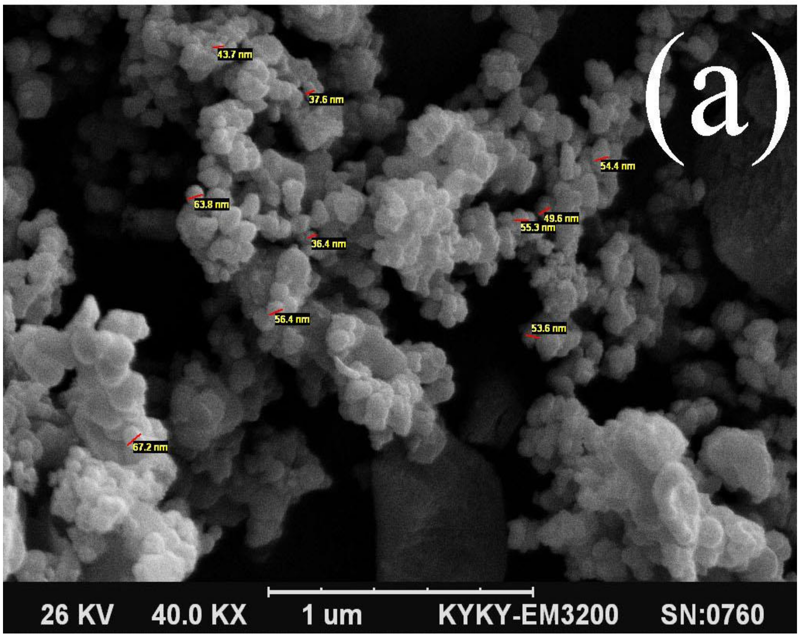

Fig. 5. SEM image of CdS nanoparticles without using any surfactants

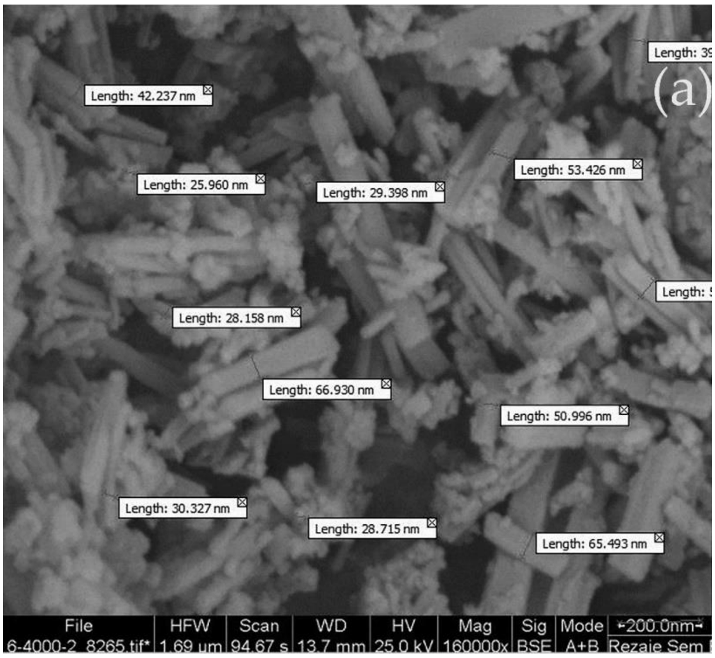

Fig. 6. SEM image of CdS nanoparticles synthesized applying CTAB

Grapefruit extract.

In both cases, nanotubes with dimensions of less than 50nm are formed; however, nanostructures synthesized using grapefruit juices have fewer dimensions of the proportion of particles synthesized by using CTAB.

SEM images of $NiFe_2O_4$-CdS nanocomposite are shown in Figs. 8 at two magnifications. The images approve formation of mono-disperse structures with average particle size of around 55 nm.

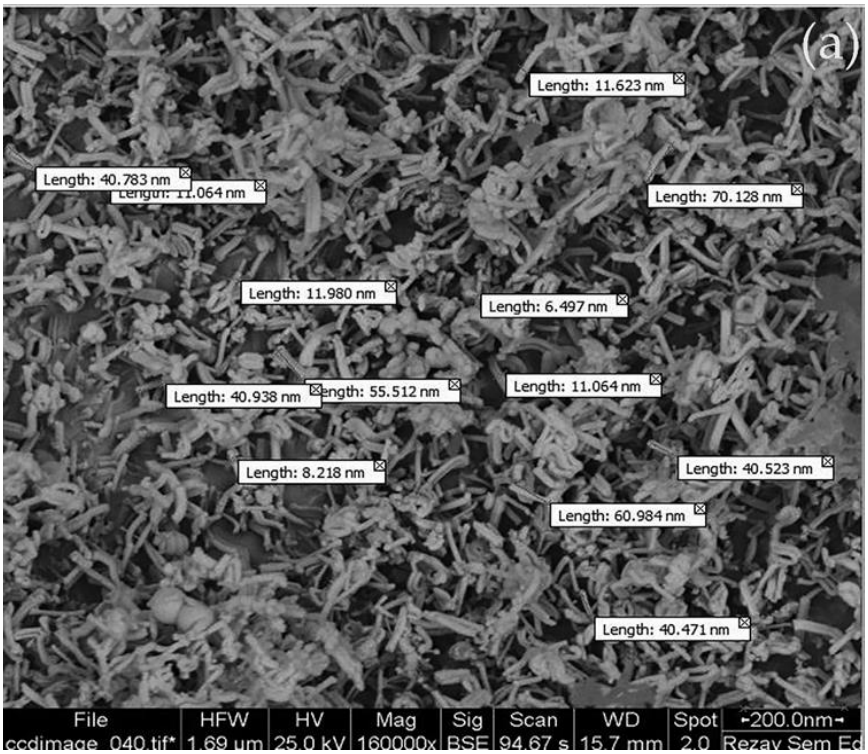

Fig. 7. SEM image of CdS nanoparticles synthesized in the presence of grapefruit extract

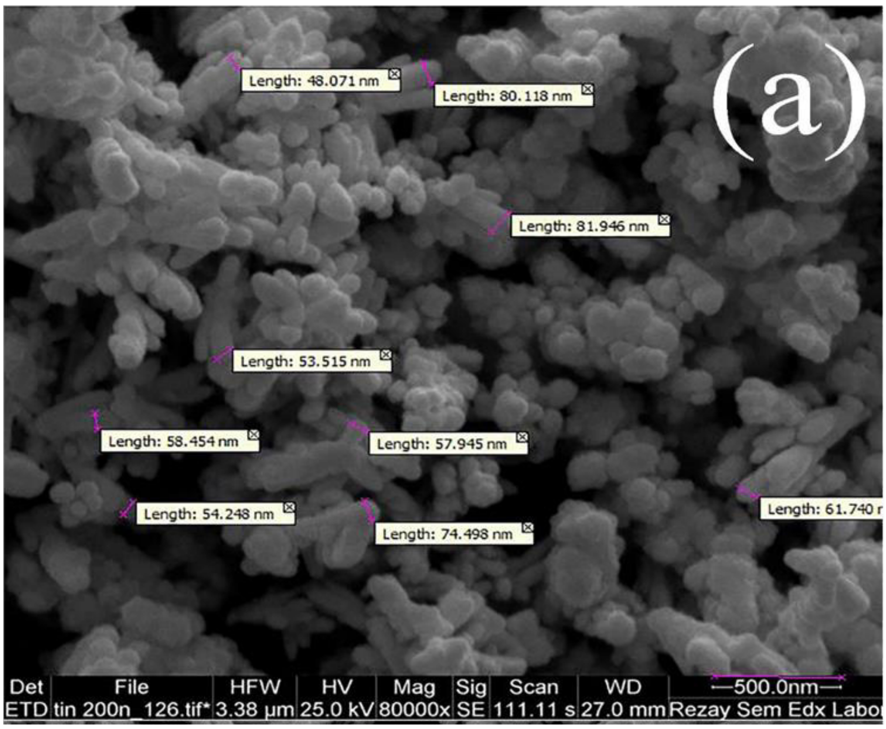

Fig. 8. SEM image of $NiFe_2O_4$- CdS nanocomposite

FT-IR analysis was used to study the type of bond and the purity of the synthesized nanocomposites of nickel ferrite -cadmium sulfide. The results of this analysis can be seen in Fig. 9. According to the FT-IR pattern, the absorption peaks in the 590 cm^{-1} range indicate the metal bond (nickel and iron) - oxygen in the ferrite composition. Also, the absorption peak in the range 47cm^{-1} indexes the

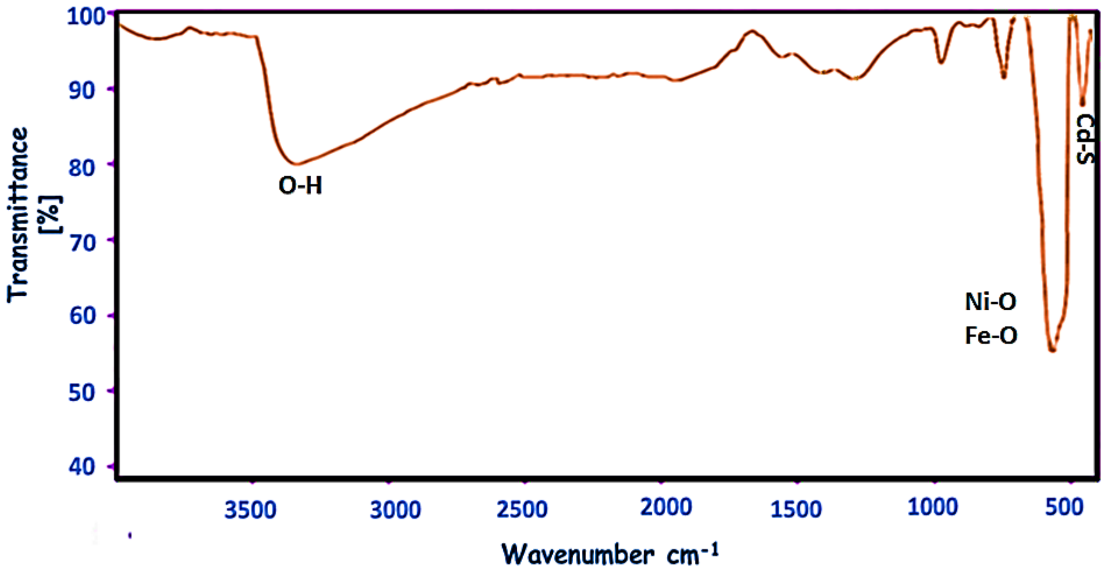

Fig. 9. FT-IR spectrum of $NiFe_2O_4$-CdS nanocomposite

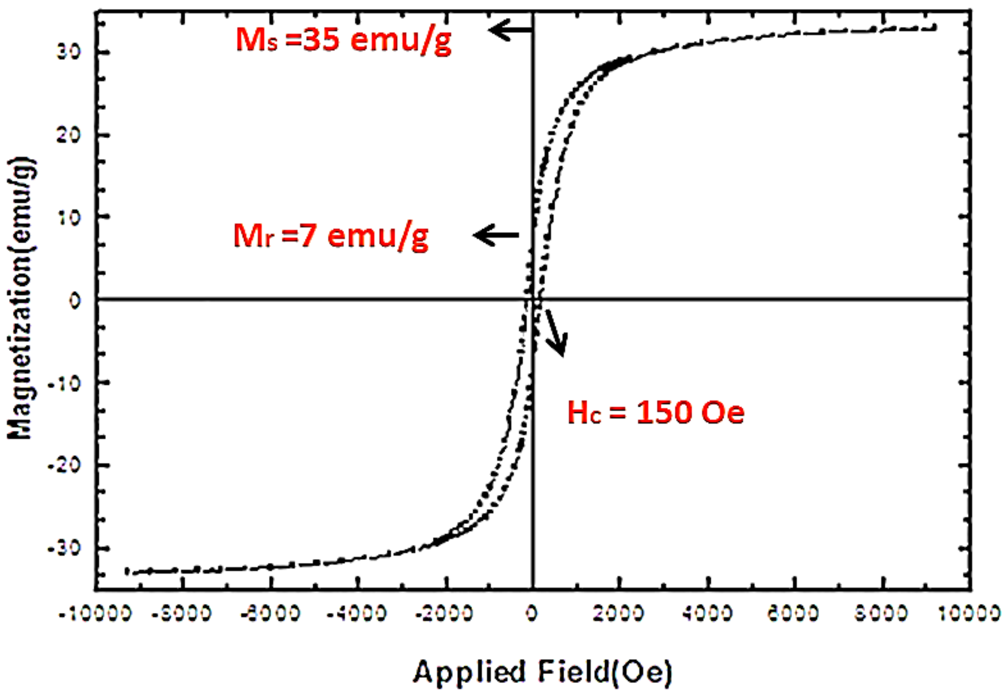

Fig. 10. VSM graph of $NiFe_2O_4$ nanoparticles

CdS bond. A peak in the range 3500 cm^{-1} is due to the O-H bond remaining on the surface of the ferrite nanoparticles.

Nickel ferrite is an inverse type of spinel; it shows high magneto crystalline anisotropy, high saturation magnetization, and unique magnetic structure. Room temperature magnetic properties of nickel ferrite samples were studied using VSM instrument. Hysteresis loops of magnetic $NiFe_2O_4$ nanoparticles and nanocomposite of $NiFe_2O_4$-CdS are shown in Figs. 10 and 11. As-synthesized magnetite nanoparticles with saturation magnetization of 35 emu/g and coercivity is 150 Oe.

M_r/M_s=0.21, the difference scale of this quantity with the number 1 represents the soft magnetism of the material. Also, the corresponding analysis of the ferri-magnetic property of the nickel ferrite nanoparticles is confirmed.

Our result also shows that prepared nanocomposite show magnetic behaviour with a saturation magnetization of 7 emu/g and coercivity is 90 Oe. As you can see, the magnetization property has dropped in comparison nickel ferrite, which can be due to the presence of cadmium sulfide in the desired nanocomposite and the coating of nickel ferrite nanoparticles by this non-magnetic material.

The energy gap of cadmium sulfide nanoparticles was calculated using ultraviolet-visible spectroscopy. According Fig. 12a an intense absorption of cadmium sulfide nanoparticles was obtained at 513.754 nm. In Fig. 12b, the energy gap was specified by the Tauc formula and Beer-Lambert law, which is as follows:

$$\alpha h\vartheta)^{n} = c(\, h\vartheta - E_g\,)\,(\frac{eV}{cm})^{n} \quad (1)$$

$$I = \log_{10}(\frac{I_0}{I}) = \alpha bc \rightarrow \alpha = \frac{A}{bc} \quad (2)$$

α is coefficient of absorption, c is constant coefficient, A is the light absorption by a solution containing nanostructure, b is the size of the

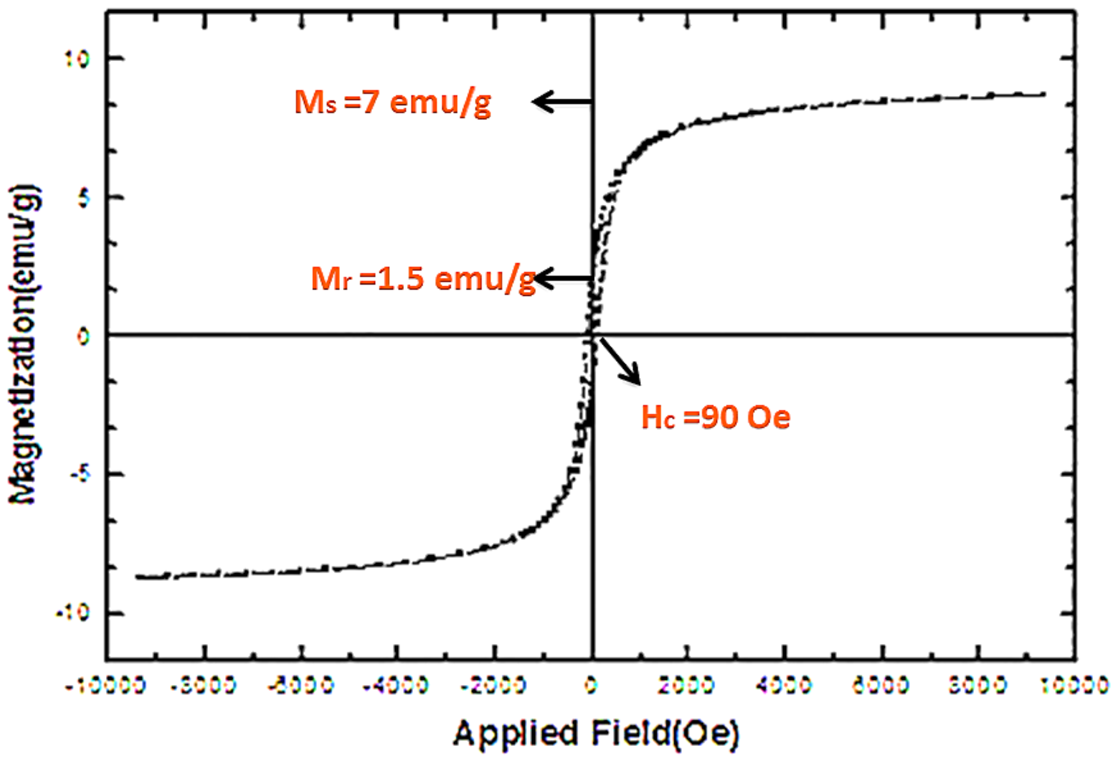

Fig.11. VSM graph of $NiFe_2O_4$ –CdS nanocomposite

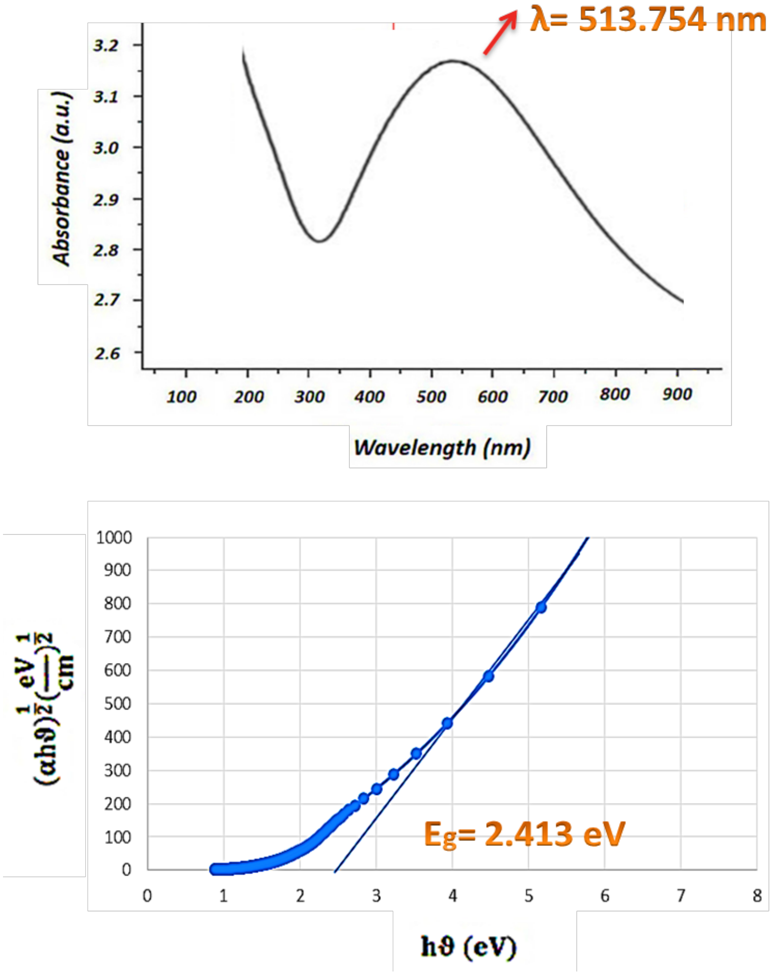

Fig. 12. UV-Vis absorption and band gap estimation of CdS nanoparticles

cuvette (cell) containing the desired solution, C is concentration of sample (with molar unit) and n for semiconductor an indirect energy gap is 1/2. From the extrapolation of this region on the longitudinal axis, the nanostructure band gap value is specified. Fig. 12b shows energy of 2.413 eV with well precision. Fig. 13 show schematic of the photoluminescence mechanism of CdS-$NiFe_2O_4$ nanostructure.

Photoluminescence property of products

The photoluminescence property of the cadmium sulfide nanoparticles synthesized by the hydrothermal method was performed using PL The cadmium sulfide nanoparticles have a significant deformity over the specified wavelength. There was no change in the wavelength, but the peak intensity increased that can owing to due to transitions between the nanoparticles conduction band with each other. Photo-luminescence of CdS prepared and reacted with Pb (II) and Hg (II), decreasing in PL peak by enhancing in Pb^{2+} and Hg^{2+} ions concentration was observed. These nanostructures introduce suitable sensor for harmful heavy metal ions detection. Orbital of Pb^{2+} and Hg^{2+} can take electron from CdS that has excitation. By junction of Pb^{2+} and Hg^{2+} ions, the fluorescence of the CdS was reduced due to electron transfer in complex compounds. By increasing the concentration of heavy metals PL

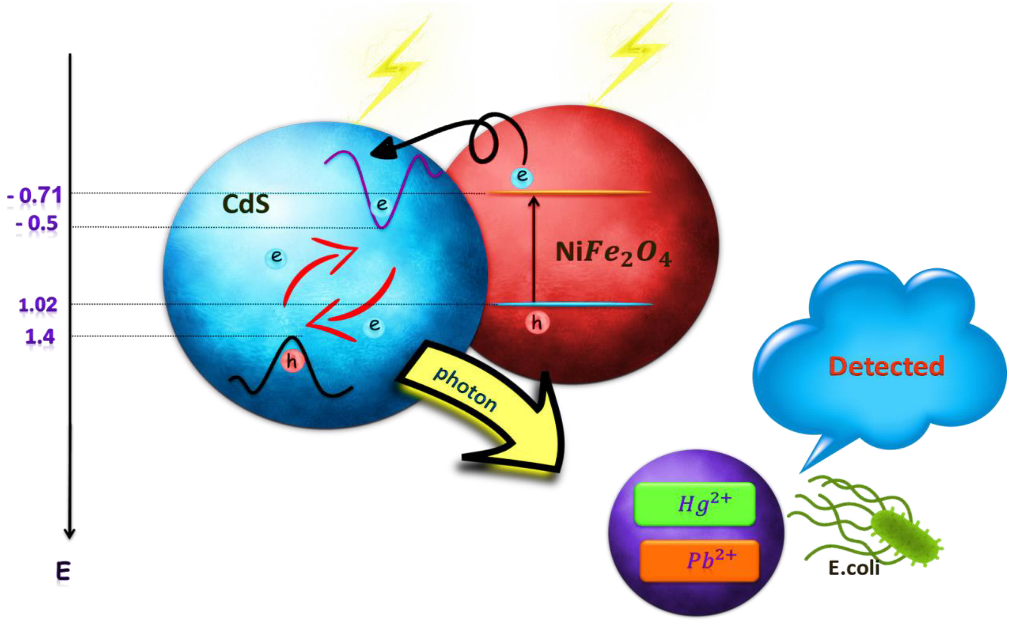

Fig. 13. Schematic of the photoluminescence mechanism of $NiFe_2O_4$-CdS nanostructure

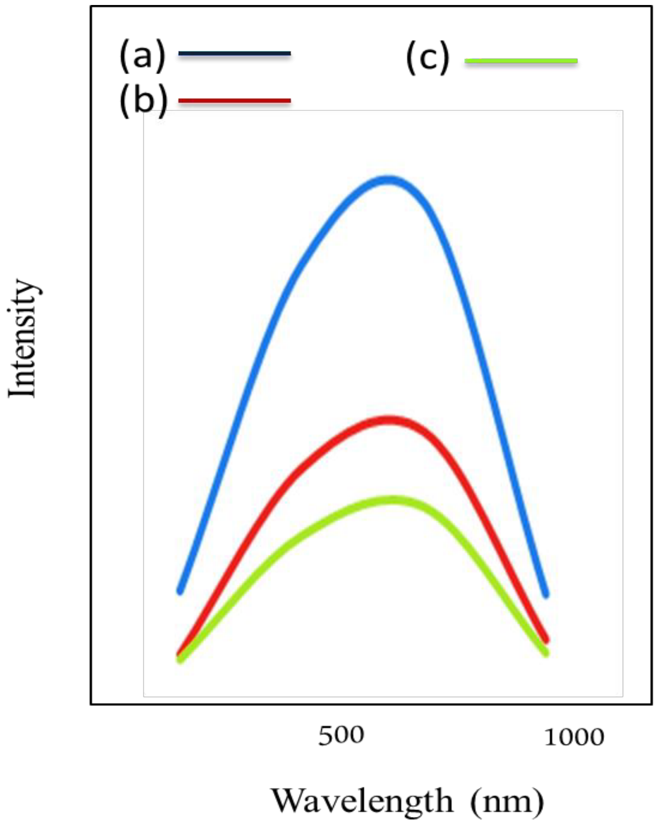

Fig. 14. (a)PL of nanocomposite by adding (b) Pb(II) (c) Hg (II)

peak is reduced further. (Fig. 14)

CONCLUSIONS

First nickel ferrite nanoparticles were synthesized via microwave-assisted and hydrothermal method. CdS nanostructure and $NiFe_2O_4$–CdS nanocomposites were then prepared via a hydrothermal method. The photoluminescence treatment of CdS nanostructure was measured using the detected of heavy metal ions. The photoluminescence activity measurements show that the CdS nanostructure result a highly active for detect of toxic ions and bacteria.

CONFLICT OF INTEREST

The authors declare that there is no conflict of interests regarding the publication of this manuscript.

REFERENCES

1. Wu Y, Wei P, Pengpumkiat S, Schumacher EA, Remcho VT. Development of a Carbon Dot (C-Dot)-Linked Immunosorbent Assay for the Detection of Human α-Fetoprotein. Anal Chem. 2015;87(16):8510-8516.
2. Zhu H, Wang X, Li Y, Wang Z, Yang F, Yang X. Microwave synthesis of fluorescent carbon nanoparticles with electrochemiluminescence properties. Chem Commun. 2009(34):5118.
3. Wang L, Kutana A, Yakobson BI. Many-body and spin-orbit effects on direct-indirect band gap transition of strained monolayer MoS_2 and WS_2. Annalen der Physik. 2014;526(9-10):L7-L12.
4. Shin MJ, Kim DH, Lim D. Photoluminescence saturation and exciton decay dynamics in transition metal dichalcogenide monolayers. Journal of the Korean Physical Society. 2014;65(12):2077-2081.
5. Anilkumar P, Wang X, Cao L, Sahu S, Liu J-H, Wang P, et al. Toward quantitatively fluorescent carbon-based “quantum” dots. Nanoscale. 2011;3(5):2023.
6. Mouri S, Miyauchi Y, Toh M, Zhao W, Eda G, Matsuda K. Nonlinear photoluminescence in atomically thin layered arising from diffusion-assisted exciton-exciton annihilation. Physical Review B. 2014;90(15).
7. Ahmadian-Fard-Fini S, Salavati-Niasari M, Ghanbari D. Hydrothermal green synthesis of magnetic Fe_3O_4-carbon dots by lemon and grape fruit extracts and as a photoluminescence sensor for detecting of E. coli bacteria. Spectrochimica Acta Part A: Molecular and Biomolecular Spectroscopy. 2018;203:481-493.
8. Ahmadian-Fard-Fini S, Ghanbari D, Salavati-Niasari M. Photoluminescence carbon dot as a sensor for detecting of Pseudomonas aeruginosa bacteria: Hydrothermal synthesis of magnetic hollow NiFe2O4-carbon dots nanocomposite material. Composites Part B: Engineering. 2019;161:564-577.
9. Yu L, Zheng Q, Wang H, Liu C, Huang X, Xiao Y. Double-Color Lanthanide Metal–Organic Framework Based Logic Device and Visual Ratiometric Fluorescence Water Microsensor for Solid Pharmaceuticals. Anal Chem. 2019;92(1):1402-1408.
10. Borah H, Gogoi S, Kalita S, Puzari P. A broad spectrum amperometric pesticide biosensor based on glutathione S-transferase immobilized on graphene oxide-gelatin matrix. J Electroanal Chem. 2018;828:116-123.
11. Kiani A, Nabiyouni G, Masoumi S, Ghanbari D. A novel magnetic $MgFe_2O_4$–$MgTiO_3$ perovskite nanocomposite: Rapid photo-degradation of toxic dyes under visible irradiation. Composites Part B: Engineering. 2019;175:107080.
12. Masoumi S, Nabiyouni G, Ghanbari D. Photo-degradation of Congored, acid brown and acid violet: photo catalyst and magnetic investigation of $CuFe_2O_4$–TiO_2–Ag nanocomposites. Journal of Materials Science: Materials in Electronics. 2016;27(10):11017-11033.
13. Chen L, Dai H, Shen Y, Bai J. Size-controlled synthesis and magnetic properties of $NiFe_2O_4$ hollow nanospheres via a gel-assistant hydrothermal route. J Alloys Compd. 2010;491(1-2):L33-L38.
14. Etminan M, Nabiyouni G, Ghanbari D. Preparation of tin ferrite–tin oxide by hydrothermal, precipitation and auto-combustion: photo-catalyst and magnetic nanocomposites for degradation of toxic azo-dyes. Journal of Materials Science: Materials in Electronics. 2017;29(3):1766-1776.
15. Masoumi S, Nabiyouni G, Ghanbari D. Photo-degradation of azo dyes: photo catalyst and magnetic investigation of $CuFe_2O_4$–TiO_2 nanoparticles and nanocomposites. Journal of Materials Science: Materials in Electronics. 2016;27(9):9962-9975.
16. Sivagurunathan P, Gibin SR. Preparation and characterization of nickel ferrite nano particles by co-precipitation method with citrate as chelating agent. Journal of Materials Science: Materials in Electronics. 2015;27(3):2601-2607.
17. Eskandari N, Nabiyouni G, Masoumi S, Ghanbari D. Preparation of a new magnetic and photo-catalyst $CoFe_2O_4$–$SrTiO_3$ perovskite nanocomposite for photo-degradation of toxic dyes under short time visible irradiation. Composites Part B: Engineering. 2019;176:107343.
18. Zor E, Morales-Narváez E, Zamora-Gálvez A, Bingol H, Ersoz M, Merkoçi A. Graphene Quantum Dots-based Photoluminescent Sensor: A Multifunctional Composite for Pesticide Detection. ACS Applied Materials & Interfaces. 2015;7(36):20272-20279.
19. Ju J, Chen W. Graphene Quantum Dots as Fluorescence Probes for Sensing Metal Ions: Synthesis and Applications. Curr Org Chem. 2015;19(12):1150-1162.
20. Chakraborti H, Sinha S, Ghosh S, Pal SK. Interfacing water soluble nanomaterials with fluorescence chemosensing: Graphene quantum dot to detect Hg^{2+} in 100% aqueous solution. Mater Lett. 2013;97:78-80.
21. Tseng Y-T, Chang H-T, Chen C-T, Chen C-H, Huang C-C. Preparation of highly luminescent mannose–gold nanodots for detection and inhibition of growth of Escherichia coli. Biosensors and Bioelectronics. 2011;27(1):95-100.
22. Xiong S, Zhou Y, Huang X, Yu R, Lai W, Xiong Y. Ultrasensitive direct competitive FLISA using highly luminescent quantum dot beads for tuning affinity of competing antigens to antibodies. Anal Chim Acta. 2017;972:94-101.